Advances in Astronomy and Space Physics, **5**, 39-42 (2015)

Nitrogen abundance in the Blue Compact Dwarf galaxies from SDSS

*K. B. Vovk**

Main Astronomical Observatory of NAS of Ukraine, Akademika Zabolotnoho str., 27, 03680 Kyiv, Ukraine

We examined all of the galaxies in the Sloan Digital Sky Survey (SDSS) Data Release 7 (DR7) to select those with a detected [O III] λ4363 emission line, which allows to derive electron temperatures in H II regions and element abundances by the direct method. We selected two sub-samples of galaxies: one with detected WR features in their spectra, and the other with the nebular He II λ4686 emission line. We confirm the increase of the N/O abundance ratio with decrease of the equivalent width EW(Hβ) of the Hβ emission line. This result is explained by gradual nitrogen enrichment of the interstellar medium by ejecta from massive stars in the most recent starburst episode.

Key words: galaxies:ISM – galaxies: starburst – galaxies: abundances – galaxies: individual: Wolf-Rayet

INTRODUCTION

Blue Compact Dwarf (BCD) galaxies, also known as HII galaxies, are small, low-mass systems which are relatively metal-poor. Most of these galaxies contain young (3–10 Myr) super stellar clusters which dominate the interstellar medium (ISM) enrichment in α-elements. The present star formation process is an important aspect of the BCD galaxies, since these galaxies prove to be excellent laboratories for studying star formation processes and physical conditions of the ISM at low metallicities with relatively small extinction problems [17]. Star formation in BCDs occurs in one or several knots in short bursts separated by long quiescent periods. A number of the least chemically evolved galaxies has been found among BCDs, for which the physical conditions in the ISM are similar to those in young galaxies at high redshifts [8, 12, 18, 24].

It is well known that the relation between the nitrogen to oxygen abundance ratio logN/O and the metallicity of the emission-line galaxies is non-linear. This is at variance with the α-element-to-oxygen abundance ratios, which do not depend on metallicity. We adopt the oxygen abundance $12+\log \mathrm{O/H}$ as a measure of metallicity. At low metallicities ($12+\log \mathrm{O/H} < 8.0$) nitrogen behaves as a primary element and the N/O ratio does not depend on metallicity, as is the case with α-elements. At higher metallicities the efficiency of nitrogen production rises and nitrogen behaves as a secondary element, and the N/O ratio increases with metallicity [10, 21]. It was found that the scatter of N/O ratio at high metallicities is higher.

However, there are low-metallicity BCDs, which have N/O ratios at a given metallicity well above the average value [6, 23]. This higher nitrogen abundance is often explained by the ISM enrichment via stellar winds of Wolf-Rayet stars (WR). This explanation is based on the simultaneous detection of increased nitrogen abundance and broad WR emission lines in integrated spectra of galaxies [5, 19, 20, 22]. It also was found in some spatially resolved observations that regions of WR emission and enhanced N abundance are coeval [14, 16]. However, this relationship is not fully confirmed.

In this paper we use a large homogeneous sample of WR-galaxies to study the correlations between the N/O ratio and other parameters (metallicity, Hβ equivalent width). Our aim is to determine the role of WR-stars in the ISM enrichment.

THE SAMPLE

We consider the sample of WR-galaxies (hereafter "WR" sample) in [3]. This sample was selected from the SDSS Data Release 7 (DR7) [1]. All spectra from the "WR" sample have blue and/or red WR features. The blue feature is a blend of emission lines N V $\lambda\lambda$4605, 4620, N III $\lambda\lambda$4634, 4640, C III λ4650, C IV λ4658 and/or broad He II λ4686. The red feature is a broad emission at C IV λ5808. We use only WR galaxies with high-excitation H II regions, where a reliable metallicity estimation by the "direct" method is possible. For this, we selected galaxies with [O III] λ4959/H$\beta > 0.7$, where the emission line [O III] λ4363 is bright enough for the reliable determination of the electron temperature and element abundances [9].

Additionally, for comparison, we consider a sam-

*agienko@mao.kiev.ua

ple of BCDs by [2] with detected nebular He II λ4686 emission ("HeII" sample). These galaxies were also selected from the SDSS DR7 [1]. A strong nebular emission of He II and no signs of WR features were present in 75% of spectra of the "HeII" sample. A nebular He II emission and the WR features were detected in the remaining 25% of spectra from the "HeII" sample. These galaxies were also included to the "WR" sample.

The positions, identifications and chemical abundances of the galaxies from both samples are included to the electronic version of the paper.

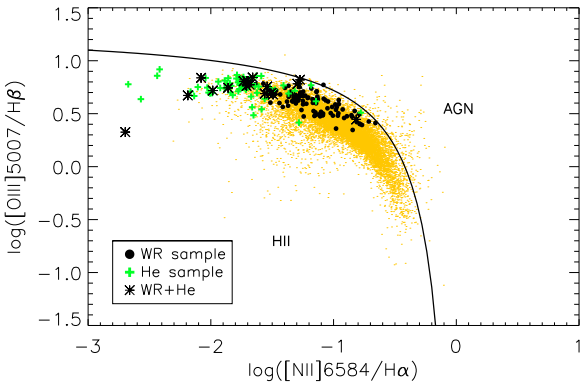

Fig. 1: The Baldwin, Phillips and Terlevich (BPT) diagnostic diagram [4] for emission-line galaxies. Solid black dots are "WR" galaxies, grey crosses are "HeII" galaxies, eight-point spikes are galaxies which are common for the two samples. Grey dots are all H II galaxies from the SDSS. A solid line by [15] separates star-forming galaxies from the AGNs.

Both samples are presented on the Baldwin, Phillips and Terlevich diagram (BPT) [4] in Fig. 1. The solid line in the Figure from [15] separates star-forming galaxies from galaxies with active nuclei (AGN). "WR" and "HeII" samples are clearly separated in the diagram, indicating that H II regions in the "HeII" galaxies are on average more metal-poor and are of higher excitation.

ELEMENT ABUNDANCES

The [O III] λ4363 emission line was observed in spectra of all galaxies from our sample. Therefore, we use the "direct" T_e-method described e. g. in [10, 13]. A two-zone photoionization model of the H II region is adopted to derive the electron temperature. According to this model, high-ionization lines [O III], [Ne III] and [Ar IV] are produced in zone with the electron temperature T_3, and low-ionization lines ([O II], [N II], [S II], [Fe III]) are produced in zone with the electron temperature T_2. The electron temperature T_3 is derived from the [O III]λ4363/(λ4959 + λ5007) flux ratio. There is no possibility to derive T_2 from our spectra. Therefore, T_2 is estimated from the relation between T_3 and T_2 [7]:

$$T_2 = 0.7T_3 + 3000.$$

Using T_3, T_2 and observed emission-line fluxes we have derived the element abundances according to [10]. We have found that oxygen abundances $12 + \log \mathrm{O/H}$ for "WR" and "HeII" samples ranged from 7.16 to 8.5, and from 7.16 to 8.4, respectively. Thus, both samples covered a wide range of metallicities.

Relations between Ar/O, Ne/O, S/O, Cl/O abundance ratios and oxygen abundances $12 + \log \mathrm{O/H}$ for all galaxies from our samples are shown in Fig. 2. The galaxies included exclusively in the "WR" sample are on average more metal-rich than those included exclusively in the "HeII" sample. Galaxies included in both samples are homogeneously distributed throughout the entire metallicity range.

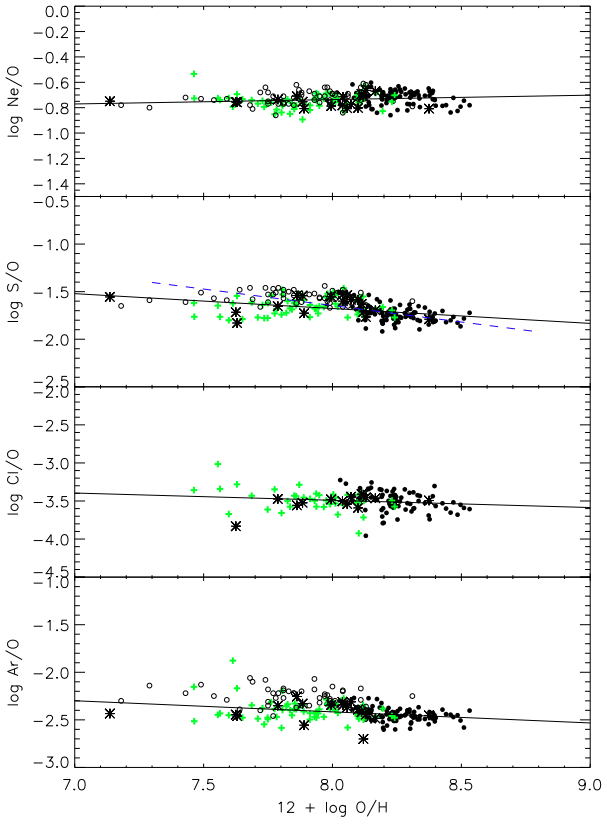

Fig. 2: Relations between Ne/O, S/O, Cl/O, Ar/O abundance ratios and oxygen abundances $12 + \log \mathrm{O/H}$. Symbols for galaxies from our samples are the same as in Fig. 1. Open circles are data from [11]. Solid lines are regressions for galaxies from both samples, dashed line is the regression for "WR" galaxies.

Distributions of Ne/O, S/O, Cl/O, Ar/O ratios on the oxygen abundance in Fig. 2 can be fitted by

linear regressions

$$\log \frac{\mathrm{Ne}}{\mathrm{O}} = (-1.013 \pm 0.129) + (0.035 \pm 0.016)X,$$

$$\log \frac{\mathrm{S}}{\mathrm{O}} = (-0.427 \pm 0.211) + (-0.156 \pm 0.026)X,$$

$$\log \frac{\mathrm{Cl}}{\mathrm{O}} = (-2.728 \pm 0.419) + (-0.095 \pm 0.051)X,$$

$$\log \frac{\mathrm{Ar}}{\mathrm{O}} = (-1.481 \pm 0.208) + (-0.117 \pm 0.025)X,$$

where $X = 12 + \log \mathrm{O/H}$.

Regressions for Ne/O and Cl/O with respective correlation coefficients of 0.15 and −0.15 are statistically not significant. Regressions for Ar/O and S/O have higher correlation coefficients of −0.31 and −0.39, respectively. This may indicate some metallicity dependence of Ar and S stellar yields compared to that of oxygen. However, as discussed by [10], atomic data for Ar and S (in particular, for dielectronic recombinations) are somewhat uncertain. These uncertainties may result in non-physical trends in the relations between Ar/O, S/O abundance ratios and metallicity.

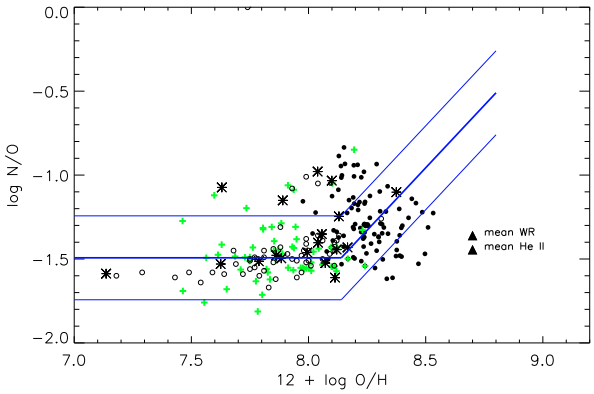

Fig. 3: Distribution of N/O abundance ratios as a function of oxygen abundances. Symbols for our samples are the same as in Fig. 1. Unshaded circles are data from [11]. The expected relation $\mathrm{N/O} - 12 + \log \mathrm{O/H}$ is shown by thick solid line, while thin lines are 0.25 dex deviations [23]. Shaded and unshaded triangles are weighted average values of N/O ratio for "WR" and "HeII" samples, respectively.

The relation between the abundance ratios N/O and the oxygen abundances is shown in Fig. 3. The N/O ratio does not depend on oxygen abundance in the galaxies with low metallicities $12 + \log \mathrm{O/H} < 8.0$. On the other hand, the N/O ratio increases and is more scattered in the galaxies with higher metallicities $12 + \log \mathrm{O/H} > 8.0$. Some galaxies in "HeII" and "WR" samples have elevated nitrogen abundances. This can be explained by the ISM enrichment with nitrogen via stellar winds from the WR stars. Despite the non-detection of WR emission lines in the low-metallicity "HeII" sample, WR stars can be present there in small numbers on much shorter timescale as compared with the galaxies with higher metallicity. The WR stars would not be visible in the integrated spectra of these galaxies, however, they may appreciably modify the nitrogen abundance.

Despite the relatively high RMS of the studied populations, the weighted mean values for the "WR" and "HeII" samples are determined with sufficient accuracy: -1.360 ± 0.006 and -1.444 ± 0.006, respectively. The difference lies within the mean values of the two populations: 0.08 ± 0.009, which translates into a formal significance equivalent to $\approx 9\sigma$.

The difference stated above illustrates the fact that the WR stars on average contribute to the overall nitrogen enrichment at levels of 20%, which is in agreement with findings of [5]. This stresses the importance of the WR stars for the chemical enrichment of the ISM of their host galaxies.

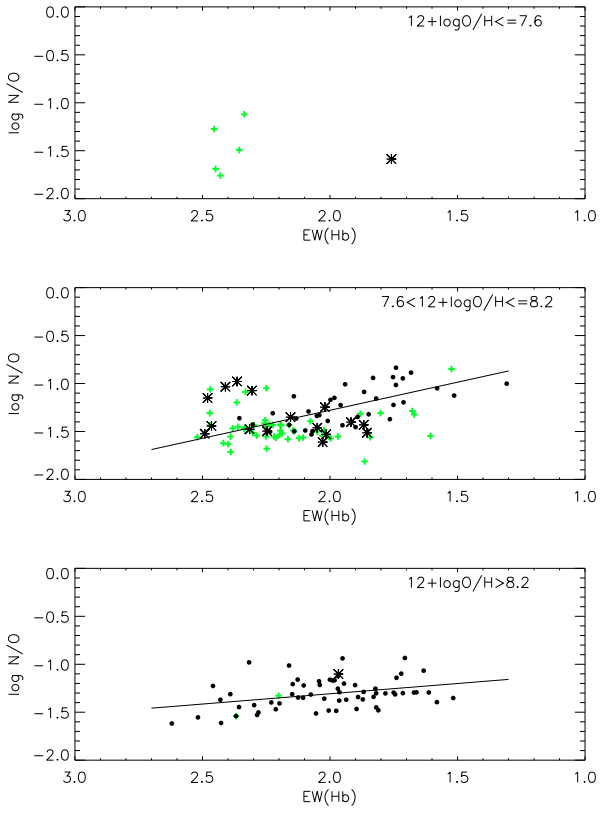

Fig. 4: Distribution of the N/O abundance ratios with the Hβ equivalent widths. Symbols are the same as in Fig. 1. Solid lines are linear-regression fits to the data.

The correlations between the N/O abundance ratios and the Hβ equivalent widths for three metallic-

ity bins are shown in Fig. 4. The number of galaxies with lowest metallicities $12 + \log \mathrm{O/H} < 7.6$ is insufficient to draw conclusions on the presence of any trends. The galaxies from the "WR" sample in the $7.6 < 12 + \log \mathrm{O/H} < 8.2$ metallicity bin do show a statistically significant correlation between the N/O ratio and EW(Hβ), with a correlation coefficient of -0.66. These data can be fitted with a linear regression

$$\log \frac{\mathrm{N}}{\mathrm{O}} = (-1.108 \pm 0.217) + (-0.585 \pm 0.111)X.$$

The Hβ equivalent width can be considered as a starburst age indicator, however applicable only for a limited period (e. g. 3–10 Myr) after the starburst ([18]). Consequently, the increase of the N/O abundance ratio with the starburst age in "WR" galaxies supports the idea that the ISM is enriched with nitrogen by WR stars during the current burst. Similar trend is also present for "WR" galaxies in the high-metallicity bin with $12 + \log \mathrm{O/H} > 8.2$:

$$\log \frac{\mathrm{N}}{\mathrm{O}} = (-0.879 \pm 0.150) + (-0.214 \pm 0.074)X.$$

However, correlation coefficient in this case is -0.34. Probably, in these galaxies with high initial nitrogen abundance, the relative increase of nitrogen $\Delta\mathrm{N/N}$, produced in the current burst, is less than in galaxies with lower metallicity. This effect was discussed in [10].

On the other hand, no correlation between N/O and EW(Hβ) was found for "HeII" galaxies.

SUMMARY

We studied chemical abundances in two samples ("WR" and "HeII") of emission-line galaxies selected in the SDSS. It was discovered that Ne/O, S/O, Cl/O and Ar/O abundance ratios do not depend on the galaxy metallicity. On the other hand, the N/O abundance ratio is increased with metallicity at $12 + \log \mathrm{O/H} > 8.0$, confirming findings in earlier studies. The N/O abundance ratio in galaxies from the "WR" sample is on average 0.08 dex higher than that of other galaxies. Furthermore, the N/O abundance ratio in galaxies from the "WR" sample increases with the age of the starburst. This effect is most significant for intermediate range of O/H. The presented above conclusions confirm the assumption that the WR stars play an important role in the ISM enrichment with nitrogen.

REFERENCES

[1] Abazajian K. N., Adelman-McCarthy J. K., Agüeros M. A. et al. 2009, ApJS, 182, 543
[2] Agienko K. B. 2013, Kinematics and Physics of Celestial Bodies, 29, 221
[3] Agienko K. B., Guseva N. G. & Izotov Y. I. 2013, Kinematics and Physics of Celestial Bodies, 29, 131
[4] Baldwin J. A., Phillips M. M. & Terlevich R. 1981, PASP, 93, 5
[5] Brinchmann J., Kunth D. & Durret F. 2008, A&A, 485, 657
[6] Chung J., Rey S.-C., Sung E.-C. et al. 2013, ApJL, 767, L15
[7] Garnett D. R. 1992, AJ, 103, 1330
[8] Guseva N. G., Izotov Y. I. & Thuan T. X. 2000, ApJ, 531, 776
[9] Izotov Y. I., Stasińska G., Guseva N. G. & Thuan T. X. 2004, A&A, 415, 87
[10] Izotov Y. I., Stasińska G., Meynet G., Guseva N. G. & Thuan T. X. 2006, A&A, 448, 955
[11] Izotov Y. I. & Thuan T. X. 1999, ApJ, 511, 639
[12] Izotov Y. I. & Thuan T. X. 2004, ApJ, 616, 768
[13] Izotov Y. I., Thuan T. X. & Lipovetsky V. A. 1994, ApJ, 435, 647
[14] James B. L., Tsamis Y. G., Barlow M. J. et al. 2009, MNRAS, 398, 2
[15] Kauffmann G., Heckman T. M., Tremonti C. et al. 2003, MNRAS, 346, 1055
[16] Kehrig C., Pérez-Montero E., Vílchez J. M. et al. 2013, MNRAS, 432, 2731
[17] Kunth D. & Östlin G. 2000, A&ARv, 10, 1
[18] Leitherer C., Schaerer D., Goldader J. D., et al. 1999, ApJS, 123, 3
[19] López-Sánchez Á. R. & Esteban C. 2010, A&A, 517, A85
[20] López-Sánchez Á. R., Esteban C., García-Rojas J., Peimbert M. & Rodríguez M. 2007, ApJ, 656, 168
[21] Mollá M., Vílchez J. M., Gavilán M. & Díaz A. I. 2006, MNRAS, 372, 1069
[22] Pagel B. E. J., Terlevich R. J. & Melnick J. 1986, PASP, 98, 1005
[23] Pilyugin L. S., Vílchez J. M., Mattsson L. & Thuan T. X. 2012, MNRAS, 421, 1624
[24] Thuan T. X. & Izotov Y. I. 2005, ApJS, 161, 240

ONLINE DATA

Table 1: WR galaxies coordinates, names.

Spectrum name	Ra	Dec	Other names
spSpec-51909-0276-197.fit	163.20268	0.0344822	[BKD2008] WR 8, SHOC 312, HIPASS J1052+00, LEDA 32664
spSpec-51662-0308-326.fit	222.0224	-1.1826967	[BKD2008] WR 25, SHOC 486
spSpec-51692-0339-083.fit	196.13445	-3.55614519	[BKD2008] WR 33, SHOC 409b
spSpec-51818-0358-472.fit	262.27731	56.88867569	[BKD2008] WR 38, SHOC 575, HS 1728+5655
spSpec-51816-0390-445.fit	5.25429	0.88002276	[BKD2008] WR 46
spSpec-51812-0394-461.fit	12.95589	0.56478471	SHOC 37, LEDA 3034, UM 283, HS 0049+0017, UCM 0049+0017
spSpec-51821-0417-513.fit	8.07747	15.00393581	[BKD2008] WR 56, SHOC 22, HS 0029+1443
spSpec-51885-0440-151.fit	123.65537	49.05001831	[BKD2008] WR 63, SHOC 193a
spSpec-51929-0473-422.fit	139.49773	1.96416581	[BKD2008] WR 73, SHOC 250
spSpec-51909-0485-306.fit	139.18349	59.7746048	[BKD2008] WR 76, Mrk 19, SBSG 0912+599, LEDA 26180, SHOC 245
spSpec-51929-0490-128.fit	164.42476	65.59439087	[BKD2008] WR 78, LEDA 2678872, SHOC 316
spSpec-52235-0501-602.fit	151.94382	2.87457108	[BKD2008] WR 82
spSpec-52017-0516-315.fit	179.30186	2.4744103	[BKD2008] WR 87, LEDA 37578, SHOC 354, Tol 1154+027, UM 469
spSpec-52312-0526-097.fit	200.54982	1.50955141	[BKD2008] WR 94
spSpec-51991-0556-224.fit	144.55624	54.47362137	[BKD2008] WR 107, LEDA 27453, SBSG 0934+546, SHOC 263
spSpec-52224-0564-216.fit	131.05931	2.43919539	[BKD2008] WR 108
spSpec-52177-0657-193.fit	13.33182	-10.40329266	[BKD2008] WR 134, SHOC 40
spSpec-52202-0695-137.fit	18.8909	-0.85865843	[BKD2008] WR 354
spSpec-52233-0753-094.fit	6.10812	14.06962395	[BKD2008] WR 143, HS 0021+1347
spSpec-52320-0782-022.fit	196.19012	62.40579987	...
spSpec-52317-0828-148.fit	129.68184	38.89736176	[BKD2008] WR 153
spSpec-52378-0843-541.fit	183.82645	5.76094913	[BKD2008] WR 156, LEDA 39188
spSpec-52374-0853-196.fit	203.71246	4.2367878	[BKD2008] WR 166, Tol 1332+044
spSpec-52411-0920-575.fit	222.02242	-1.18270004	[BKD2008] WR 182, SHOC 486
spSpec-52672-0934-369.fit	131.64333	36.43912506	[BKD2008] WR 183, Mrk 627, HS 0843+3637, LEDA 24655
spSpec-52407-0946-618.fit	155.43515	56.92210388	[BKD2008] WR 188, NGC 3206
spSpec-52431-0978-118.fit	259.72269	30.19338799	[BKD2008] WR 358, [BKD2008] WR 202, LEDA 97542, IRAS 17169+3014
spSpec-52636-0999-517.fit	158.36887	7.13382339	[BKD2008] WR 204, IRAS 10308+0723, LEDA 31208
spSpec-52709-1015-003.fit	175.88794	53.50019073	[BKD2008] WR 212, Mrk 1451, SBSG 1140+537, IRAS Z11408+5346
spSpec-52707-1039-119.fit	196.86958	54.4471283	[BKD2008] WR 216, SBSG 1305+547, LEDA 2816039
spSpec-52674-1164-298.fit	223.679	52.42914963	[BKD2008] WR 228, LEDA 2414734, SBSG 1453+526, LEDA 2414734
spSpec-52734-1233-136.fit	189.3904	8.88216496	[BKD2008] WR 235, Tol 1235+091, IRAS F12350+0909
spSpec-52932-1267-384.fit	125.97903	28.10604286	[BKD2008] WR 238, IRAS F08208+2816
spSpec-52765-1277-031.fit	149.9655	38.55857086	HS 0956+3847
spSpec-52731-1288-390.fit	217.55081	45.54233932	[BKD2008] WR 243, LEDA 51821
spSpec-52757-1305-269.fit	145.73643	9.47118378	[BKD2008] WR 245
spSpec-52797-1323-002.fit	210.75487	54.24150085	[BKD2008] WR 253, NGC 5455
spSpec-52797-1323-008.fit	210.62744	54.26935196	[BKD2008] WR 254, NGC 5457 444
spSpec-52762-1325-412.fit	212.4865	54.94691467	[BKD2008] WR 264, LEDA 2816082, SBSG 1408+551A
spSpec-52781-1332-063.fit	234.59167	45.80195236	[BKD2008] WR 266, HS 1536+4557
spSpec-53003-1360-634.fit	159.76686	41.66136932	[BKD2008] WR 272
spSpec-53047-1361-221.fit	159.75157	41.6690979	[BKD2008] WR 273
spSpec-53050-1362-617.fit	165.10378	43.01998138	[BKD2008] WR 275, IRAS F10575+4317
spSpec-53063-1366-083.fit	173.72063	44.00485229	[BKD2008] WR 277
spSpec-52821-1371-059.fit	187.05775	44.11956406	[BKD2008] WR 283
spSpec-53118-1387-458.fit	230.65875	33.52661514	[BKD2008] WR 291, LEDA 84586
spSpec-53112-1452-008.fit	187.62372	41.65457535	[BKD2008] WR 304
spSpec-53112-1452-009.fit	187.64362	41.64217758	[BKD2008] WR 305, NGC 4490, KPG 341, LEDA 41333, UGC 7651
spSpec-53112-1452-011.fit	187.61806	41.68946457	[BKD2008] WR 306, NGC 4485, LEDA 41326, UGC 7648
spSpec-53090-1454-299.fit	187.64352	41.64035416	[BKD2008] WR 309, NGC 4490, KPG 341, LEDA 41333, UGC 7651
spSpec-52998-1596-479.fit	149.33862	36.87910843	[BKD2008] WR 322, LEDA 87430
spSpec-53117-1602-380.fit	163.32162	12.77744198	[BKD2008] WR 324
spSpec-53120-1614-499.fit	185.93529	12.47833347	[BKD2008] WR 329, IC 3258, KUG 1221+127, LEDA 40264, UGC 7470
spSpec-53474-1628-185.fit	189.25945	6.92527914	[BKD2008] WR 364, IC 3591, Mrk 1329, Tol 1234+072, UGC 7790
spSpec-53473-1695-627.fit	195.33026	12.66652012	[BKD2008] WR 377
spSpec-53061-1745-196.fit	153.11259	12.34374905	[BKD2008] WR 340
spSpec-53463-1763-094.fit	180.13925	13.71888542	[BKD2008] WR 386
spSpec-53524-1851-225.fit	239.38461	23.34734154	[BKD2008] WR 394
spSpec-53566-1854-551.fit	246.99287	20.24558449	[BKD2008] WR 458
spSpec-53315-1922-588.fit	121.58123	19.82425308	[BKD2008] WR 396
spSpec-53349-1929-230.fit	127.66406	22.25099754	[BKD2008] WR 397
spSpec-53388-1948-132.fit	149.38692	33.6197319	[BKD2008] WR 402, IC 2524, LEDA 28758, Mrk 411, ZW I 524

Continued on next page

Table 1 – continued from previous page

Spectrum name	Ra	Dec	Other names
spSpec-53433-1949-480.fit	149.49866	32.23965454	[BKD2008] WR 403, Mrk 412, KUG 0955+324, LEDA 28791
spSpec-53321-1962-077.fit	323.65753	11.4194994	[BKD2008] WR 404, LEDA 66989
spSpec-53431-1979-074.fit	170.77901	30.47892189	[BKD2008] WR 407, [BKD2008] WR 514, KUG 1120+307, LEDA 34952
spSpec-53463-1981-438.fit	161.84837	30.36230278	[BKD2008] WR 409, LEDA 32228
spSpec-53446-1991-584.fit	179.38222	32.34171295	[BKD2008] WR 412, LEDA 200277, NGC 3991, UGC 6933
spSpec-53800-2018-096.fit	195.97685	37.2338562	[BKD2008] WR 471, LEDA 45141
spSpec-53818-2028-494.fit	206.77881	34.94005966	[BKD2008] WR 478, HS 1344+3511, LEDA 84048
spSpec-53848-2031-048.fit	194.60136	35.25047684	[BKD2008] WR 479
spSpec-53815-2032-243.fit	198.32692	36.20294189	[BKD2008] WR 480, UGC 8303, DDO 166, HS 1311+3628, LEDA 45927
spSpec-53401-2086-458.fit	136.35976	25.55071259	[BKD2008] WR 425, UGC 4764, LEDA 25512
spSpec-53463-2090-550.fit	163.12167	36.61384583	[BKD2008] WR 427, NGC 3432, LEDA 32643, UGC 5986
spSpec-53534-2112-557.fit	201.45593	33.06510544	[BKD2008] WR 440, HS 1323+3319, LEDA 46979
spSpec-53491-2147-514.fit	161.33508	9.3969717	[BKD2008] WR 443, Tol 1042+097
spSpec-53557-2171-183.fit	238.51884	21.582407	[BKD2008] WR 502
spSpec-53566-2202-017.fit	246.96321	13.58714867	[BKD2008] WR 505
spSpec-53880-2208-306.fit	245.46906	15.3155508	...
spSpec-53789-2212-255.fit	165.89182	25.40454102	...
spSpec-53793-2223-629.fit	179.52039	27.87424469	[BKD2008] WR 515, NGC 4004, LEDA 37654, Mrk 432, UGC 6950
spSpec-54205-2238-091.fit	191.73088	26.56428719	Mrk 1335, KUG 1244+268, LEDA 43121, UGCA 298
spSpec-53757-2347-133.fit	152.74524	25.50438499	[BKD2008] WR 539, LEDA 139257
spSpec-53792-2355-229.fit	160.88181	24.96635056	[BKD2008] WR 541
spSpec-53792-2355-574.fit	162.1842	26.05364609	[BKD2008] WR 544, Mrk 727, LEDA 32329
spSpec-53741-2366-124.fit	156.01146	21.08056641	[BKD2008] WR 555, LEDA 30483
spSpec-54097-2478-585.fit	162.20634	21.01042366	...
spSpec-54175-2495-240.fit	169.57188	18.84710503	UGC 6320, HIPASS J1118+18, LEDA 34556
spSpec-54178-2500-084.fit	172.30898	20.58111382	LEDA 35380
spSpec-54141-2513-309.fit	177.02271	21.82926369	Mrk 1459, LEDA 36837
spSpec-54568-2524-146.fit	241.61473	13.92996693	...
spSpec-54084-2574-323.fit	131.84924	11.36525917	...
spSpec-54095-2583-062.fit	149.17703	15.63648224	Mrk 712, UGC 5342, LEDA 28707
spSpec-54140-2591-226.fit	156.28389	17.15276718	NGC 3239, LEDA 30560, UGC 5637
spSpec-54476-2603-512.fit	196.6996	17.64916611	...
spSpec-54154-2606-474.fit	202.31898	17.00583458	...
spSpec-54476-2610-421.fit	183.8275	20.64075661	Mrk 1315, KUG 1212+209B, LEDA 39187
spSpec-54481-2613-507.fit	189.62473	19.98926735	...
spSpec-54272-2744-090.fit	210.94344	14.86810493	Mrk 802, KUG 1401+151, LEDA 50114
spSpec-54523-2758-062.fit	213.63451	17.98318481	...

Table 2: WR galaxies abundances.

Spectrum name	12 + log O/H	log N/O	log Ne/O	log S/O	log Ar/O	log Cl/O
spSpec-51909-0276-197.fit	8.377 ± 0.101	-1.395 ± 0.128	-0.672 ± 0.205	-1.712 ± 0.169	-2.471 ± 0.127	-3.740 ± 0.579
spSpec-51662-0308-326.fit	8.052 ± 0.057	-1.365 ± 0.076	-0.751 ± 0.114	-1.619 ± 0.105	-2.338 ± 0.074	-3.272 ± 0.237
spSpec-51692-0339-083.fit	8.337 ± 0.038	-1.533 ± 0.050	-0.738 ± 0.075	-1.710 ± 0.070	-2.438 ± 0.051	-3.428 ± 0.136
spSpec-51818-0358-472.fit	8.211 ± 0.033	-1.177 ± 0.044	-0.740 ± 0.062	-1.756 ± 0.075	-2.405 ± 0.044	-3.368 ± 0.165
spSpec-51816-0390-445.fit	8.165 ± 0.042	-1.225 ± 0.055	-0.671 ± 0.080	-1.738 ± 0.086	-2.509 ± 0.056	-3.478 ± 0.253
spSpec-51812-0394-461.fit	8.030 ± 0.063	-1.223 ± 0.083	-0.775 ± 0.134	-1.505 ± 0.115	-2.297 ± 0.083	-3.225 ± 0.294
spSpec-51821-0417-513.fit	8.107 ± 0.030	-1.435 ± 0.041	-0.740 ± 0.057	-1.587 ± 0.060	-2.368 ± 0.041	-3.466 ± 0.215
spSpec-51885-0440-151.fit	8.302 ± 0.036	-1.398 ± 0.048	-0.721 ± 0.070	-1.680 ± 0.064	-2.593 ± 0.048	-3.538 ± 0.164
spSpec-51929-0473-422.fit	8.094 ± 0.092	-1.052 ± 0.120	-0.683 ± 0.189	-1.691 ± 0.180	-2.370 ± 0.118	...
spSpec-51909-0485-306.fit	8.314 ± 0.072	-1.293 ± 0.092	-0.772 ± 0.148	-1.731 ± 0.120	-2.453 ± 0.092	-3.386 ± 0.222
spSpec-51929-0490-128.fit	8.292 ± 0.042	-1.449 ± 0.056	-0.819 ± 0.078	-1.690 ± 0.090	-2.402 ± 0.084	...
spSpec-52235-0501-602.fit	8.192 ± 0.042	-1.489 ± 0.056	-0.726 ± 0.080	-1.722 ± 0.087	-2.465 ± 0.094	-3.444 ± 0.238
spSpec-52017-0516-315.fit	7.976 ± 0.043	-1.156 ± 0.057	-0.737 ± 0.086	-1.649 ± 0.086	-2.336 ± 0.057	...
spSpec-52312-0526-097.fit	8.387 ± 0.077	-1.202 ± 0.099	-0.684 ± 0.157	-1.800 ± 0.132	-2.485 ± 0.099	...
spSpec-51991-0556-224.fit	8.127 ± 0.049	-1.087 ± 0.065	-0.700 ± 0.096	-1.799 ± 0.113	-2.474 ± 0.066	-3.619 ± 0.449
spSpec-52224-0564-216.fit	8.195 ± 0.042	-1.170 ± 0.056	-0.706 ± 0.077	-1.835 ± 0.099	-2.523 ± 0.106	-3.792 ± 0.487
spSpec-52177-0657-193.fit	8.142 ± 0.099	-1.004 ± 0.130	-0.783 ± 0.199	-1.726 ± 0.212	-2.472 ± 0.129	...
spSpec-52202-0695-137.fit	8.376 ± 0.027	-1.446 ± 0.036	-0.705 ± 0.054	-1.767 ± 0.050	-2.418 ± 0.044	-3.513 ± 0.095
spSpec-52233-0753-094.fit	8.389 ± 0.071	-1.481 ± 0.093	-0.669 ± 0.141	-1.820 ± 0.149	-2.426 ± 0.091	...
spSpec-52320-0782-022.fit	8.304 ± 0.098	-1.098 ± 0.125	-0.674 ± 0.197	-1.766 ± 0.176	-2.538 ± 0.126	...
spSpec-52317-0828-148.fit	8.199 ± 0.040	-1.292 ± 0.053	-0.699 ± 0.075	-1.802 ± 0.086	-2.603 ± 0.109	-3.787 ± 0.452
spSpec-52378-0843-541.fit	8.247 ± 0.067	-1.295 ± 0.085	-0.717 ± 0.136	-1.742 ± 0.127	-2.447 ± 0.130	-3.446 ± 0.289
spSpec-52374-0853-196.fit	8.299 ± 0.078	-1.365 ± 0.102	-0.679 ± 0.155	-1.636 ± 0.147	-2.418 ± 0.101	...

Continued on next page

Table 2 – continued from previous page

Spectrum name	12 + log O/H	log N/O	log Ne/O	log S/O	log Ar/O	log Cl/O
spSpec-52411-0920-575.fit	8.098 ± 0.025	-1.434 ± 0.037	-0.728 ± 0.043	-1.588 ± 0.055	-2.443 ± 0.055	-3.515 ± 0.185
spSpec-52672-0934-369.fit	8.239 ± 0.044	-1.342 ± 0.058	-0.699 ± 0.085	-1.722 ± 0.083	-2.451 ± 0.057	...
spSpec-52407-0946-618.fit	8.235 ± 0.042	-1.425 ± 0.056	-0.718 ± 0.083	-1.760 ± 0.083	-2.446 ± 0.080	-3.425 ± 0.177
spSpec-52431-0978-118.fit	8.441 ± 0.102	-1.140 ± 0.128	-0.778 ± 0.212	-1.821 ± 0.167	-2.441 ± 0.128	-3.599 ± 0.318
spSpec-52636-0999-517.fit	8.290 ± 0.111	-0.935 ± 0.141	-0.771 ± 0.228	-1.751 ± 0.177	-2.422 ± 0.140	-3.529 ± 0.361
spSpec-52709-1015-003.fit	8.225 ± 0.055	-1.339 ± 0.071	-0.678 ± 0.108	-1.729 ± 0.108	-2.434 ± 0.071	...
spSpec-52707-1039-119.fit	8.373 ± 0.046	-1.483 ± 0.060	-0.648 ± 0.091	-1.846 ± 0.092	-2.547 ± 0.061	-3.691 ± 0.300
spSpec-52674-1164-298.fit	8.017 ± 0.066	-1.348 ± 0.089	-0.681 ± 0.132	-1.506 ± 0.119	-2.354 ± 0.086	...
spSpec-52734-1233-136.fit	8.152 ± 0.068	-0.928 ± 0.087	-0.815 ± 0.141	-1.710 ± 0.127	-2.350 ± 0.087	...
spSpec-52932-1267-384.fit	8.194 ± 0.041	-1.008 ± 0.054	-0.683 ± 0.080	-1.833 ± 0.083	-2.468 ± 0.053	-3.420 ± 0.186
spSpec-52765-1277-031.fit	8.262 ± 0.084	-1.124 ± 0.109	-0.711 ± 0.166	-1.639 ± 0.148	-2.384 ± 0.107	...
spSpec-52731-1288-390.fit	8.431 ± 0.047	-1.504 ± 0.061	-0.755 ± 0.093	-1.741 ± 0.089	-2.538 ± 0.061	...
spSpec-52757-1305-269.fit	8.241 ± 0.023	-1.541 ± 0.032	-0.702 ± 0.045	-1.771 ± 0.045	-2.476 ± 0.045	-3.573 ± 0.125
spSpec-52797-1323-002.fit	8.565 ± 0.025	-1.336 ± 0.032	-0.791 ± 0.053	-1.780 ± 0.044	-2.558 ± 0.041	-3.620 ± 0.074
spSpec-52797-1323-008.fit	8.533 ± 0.043	-1.224 ± 0.054	-0.776 ± 0.092	-1.722 ± 0.070	-2.405 ± 0.062	-3.604 ± 0.116
spSpec-52762-1325-412.fit	8.241 ± 0.037	-1.160 ± 0.051	-0.725 ± 0.065	-1.679 ± 0.081	-2.504 ± 0.087	-3.539 ± 0.250
spSpec-52781-1332-063.fit	8.140 ± 0.104	-1.018 ± 0.134	-0.711 ± 0.212	-1.651 ± 0.200	-2.271 ± 0.133	...
spSpec-53003-1360-634.fit	8.299 ± 0.029	-1.370 ± 0.039	-0.773 ± 0.056	-1.676 ± 0.056	-2.392 ± 0.050	-3.393 ± 0.106
spSpec-53047-1361-221.fit	8.280 ± 0.028	-1.419 ± 0.037	-0.736 ± 0.057	-1.707 ± 0.055	-2.344 ± 0.039	-3.510 ± 0.132
spSpec-53050-1362-617.fit	8.128 ± 0.051	-1.372 ± 0.068	-0.731 ± 0.102	-1.728 ± 0.110	-2.487 ± 0.134	-3.428 ± 0.342
spSpec-53063-1366-083.fit	8.233 ± 0.046	-1.379 ± 0.061	-0.690 ± 0.086	-1.682 ± 0.092	-2.417 ± 0.060	-3.375 ± 0.207
spSpec-52821-1371-059.fit	8.555 ± 0.024	-1.565 ± 0.031	-0.797 ± 0.049	-1.761 ± 0.043	-2.425 ± 0.033	-3.558 ± 0.073
spSpec-53118-1387-458.fit	8.131 ± 0.108	-0.889 ± 0.139	-0.789 ± 0.235	-1.890 ± 0.177	-2.501 ± 0.136	-3.960 ± 1.093
spSpec-53112-1452-008.fit	8.339 ± 0.064	-1.348 ± 0.082	-0.794 ± 0.131	-1.808 ± 0.112	-2.460 ± 0.082	-3.432 ± 0.190
spSpec-53112-1452-009.fit	8.389 ± 0.062	-1.359 ± 0.079	-0.733 ± 0.127	-1.770 ± 0.102	-2.476 ± 0.079	-3.438 ± 0.165
spSpec-53112-1452-011.fit	8.344 ± 0.049	-1.452 ± 0.063	-0.707 ± 0.100	-1.801 ± 0.085	-2.506 ± 0.063	-3.495 ± 0.154
spSpec-53090-1454-299.fit	8.497 ± 0.047	-1.469 ± 0.060	-0.792 ± 0.097	-1.865 ± 0.080	-2.507 ± 0.075	-3.550 ± 0.134
spSpec-52998-1596-479.fit	8.150 ± 0.092	-0.833 ± 0.118	-0.813 ± 0.192	-1.708 ± 0.161	-2.392 ± 0.118	-3.254 ± 0.261
spSpec-53117-1602-380.fit	8.141 ± 0.040	-1.531 ± 0.064	-0.758 ± 0.068	-1.535 ± 0.098	-2.392 ± 0.098	-3.344 ± 0.269
spSpec-53120-1614-499.fit	8.190 ± 0.045	-1.310 ± 0.059	-0.783 ± 0.092	-1.686 ± 0.078	-2.324 ± 0.059	-3.353 ± 0.144
spSpec-53474-1628-185.fit	8.359 ± 0.023	-1.612 ± 0.032	-0.706 ± 0.042	-1.667 ± 0.042	-2.491 ± 0.039	-3.527 ± 0.090
spSpec-53473-1695-627.fit	8.208 ± 0.074	-0.936 ± 0.094	-0.765 ± 0.149	-1.796 ± 0.133	-2.441 ± 0.094	-3.655 ± 0.467
spSpec-53061-1745-196.fit	8.085 ± 0.028	-1.501 ± 0.044	-0.719 ± 0.049	-1.535 ± 0.065	-2.271 ± 0.054	-3.434 ± 0.203
spSpec-53463-1763-094.fit	8.236 ± 0.036	-0.981 ± 0.049	-0.751 ± 0.065	-1.681 ± 0.075	-2.484 ± 0.076	-3.485 ± 0.197
spSpec-53524-1851-225.fit	8.314 ± 0.039	-1.347 ± 0.050	-0.689 ± 0.077	-1.778 ± 0.073	-2.477 ± 0.073	-3.599 ± 0.206
spSpec-53566-1854-551.fit	8.242 ± 0.050	-1.300 ± 0.065	-0.659 ± 0.099	-1.881 ± 0.104	-2.598 ± 0.066	-3.421 ± 0.217
spSpec-53315-1922-588.fit	8.307 ± 0.059	-1.288 ± 0.077	-0.706 ± 0.116	-1.762 ± 0.118	-2.458 ± 0.077	-3.637 ± 0.410
spSpec-53349-1929-230.fit	8.120 ± 0.052	-1.338 ± 0.069	-0.737 ± 0.103	-1.678 ± 0.102	-2.356 ± 0.068	-3.435 ± 0.301
spSpec-53388-1948-132.fit	8.281 ± 0.069	-1.351 ± 0.090	-0.648 ± 0.130	-1.725 ± 0.137	-2.454 ± 0.086	-3.347 ± 0.289
spSpec-53433-1949-480.fit	8.400 ± 0.080	-1.301 ± 0.101	-0.784 ± 0.165	-1.805 ± 0.137	-2.479 ± 0.102	-3.566 ± 0.295
spSpec-53321-1962-077.fit	8.238 ± 0.098	-1.291 ± 0.125	-0.678 ± 0.199	-1.733 ± 0.164	-2.422 ± 0.125	-3.489 ± 0.397
spSpec-53431-1979-074.fit	8.217 ± 0.062	-1.161 ± 0.080	-0.707 ± 0.124	-1.710 ± 0.105	-2.375 ± 0.079	-3.498 ± 0.257
spSpec-53463-1981-438.fit	8.262 ± 0.041	-1.255 ± 0.054	-0.657 ± 0.081	-1.766 ± 0.082	-2.469 ± 0.054	-3.506 ± 0.222
spSpec-53446-1991-584.fit	8.396 ± 0.077	-1.313 ± 0.098	-0.734 ± 0.159	-1.815 ± 0.131	-2.452 ± 0.098	-3.303 ± 0.178
spSpec-53800-2018-096.fit	8.104 ± 0.029	-1.390 ± 0.040	-0.674 ± 0.054	-1.696 ± 0.068	-2.426 ± 0.067	-3.492 ± 0.244
spSpec-53818-2028-494.fit	8.193 ± 0.074	-0.942 ± 0.093	-0.735 ± 0.155	-1.918 ± 0.114	-2.472 ± 0.092	-3.704 ± 0.341
spSpec-53848-2031-048.fit	8.193 ± 0.061	-1.321 ± 0.079	-0.693 ± 0.118	-1.724 ± 0.120	-2.379 ± 0.078	...
spSpec-53815-2032-243.fit	8.284 ± 0.022	-1.554 ± 0.031	-0.695 ± 0.043	-1.765 ± 0.042	-2.445 ± 0.038	-3.613 ± 0.106
spSpec-53401-2086-458.fit	8.173 ± 0.072	-1.149 ± 0.094	-0.840 ± 0.149	-1.580 ± 0.133	-2.281 ± 0.094	-3.487 ± 0.406
spSpec-53463-2090-550.fit	8.225 ± 0.045	-1.513 ± 0.060	-0.654 ± 0.083	-1.687 ± 0.084	-2.466 ± 0.057	-3.569 ± 0.286
spSpec-53534-2112-557.fit	8.197 ± 0.030	-1.497 ± 0.043	-0.679 ± 0.055	-1.757 ± 0.070	-2.583 ± 0.084	-3.596 ± 0.240
spSpec-53491-2147-514.fit	8.221 ± 0.045	-1.316 ± 0.060	-0.726 ± 0.085	-1.739 ± 0.090	-2.493 ± 0.101	-3.537 ± 0.284
spSpec-53557-2171-183.fit	8.330 ± 0.054	-1.218 ± 0.070	-0.672 ± 0.110	-1.798 ± 0.096	-2.495 ± 0.070	-3.424 ± 0.180
spSpec-53566-2202-017.fit	8.107 ± 0.046	-1.329 ± 0.061	-0.712 ± 0.091	-1.658 ± 0.088	-2.446 ± 0.061	-3.332 ± 0.214
spSpec-53880-2208-306.fit	8.226 ± 0.037	-1.016 ± 0.050	-0.858 ± 0.069	-1.595 ± 0.075	-2.452 ± 0.050	-3.434 ± 0.206
spSpec-53789-2212-255.fit	8.306 ± 0.065	-1.216 ± 0.084	-0.676 ± 0.127	-1.744 ± 0.121	-2.526 ± 0.085	...
spSpec-53793-2223-629.fit	8.485 ± 0.107	-1.221 ± 0.132	-0.826 ± 0.230	-1.827 ± 0.156	-2.451 ± 0.133	-3.680 ± 0.260
spSpec-54205-2238-091.fit	8.252 ± 0.072	-1.294 ± 0.089	-0.819 ± 0.149	-1.785 ± 0.112	-2.409 ± 0.087	-3.744 ± 0.387
spSpec-53757-2347-133.fit	8.184 ± 0.070	-1.196 ± 0.092	-0.657 ± 0.132	-1.608 ± 0.144	-2.371 ± 0.147	-3.346 ± 0.390
spSpec-53792-2355-229.fit	8.322 ± 0.060	-1.312 ± 0.078	-0.683 ± 0.120	-1.719 ± 0.106	-2.463 ± 0.078	...
spSpec-53792-2355-574.fit	8.340 ± 0.090	-1.070 ± 0.114	-0.727 ± 0.185	-1.899 ± 0.142	-2.497 ± 0.113	...
spSpec-53741-2366-124.fit	8.168 ± 0.031	-1.499 ± 0.043	-0.685 ± 0.057	-1.686 ± 0.064	-2.470 ± 0.070	...
spSpec-54097-2478-585.fit	8.247 ± 0.055	-1.467 ± 0.073	-0.675 ± 0.106	-1.822 ± 0.131	-2.511 ± 0.137	-3.500 ± 0.364
spSpec-54175-2495-240.fit	8.427 ± 0.096	-1.255 ± 0.120	-0.786 ± 0.205	-1.703 ± 0.147	-2.393 ± 0.121	-3.530 ± 0.226
spSpec-54178-2500-084.fit	8.404 ± 0.032	-1.550 ± 0.045	-0.764 ± 0.068	-1.720 ± 0.064	-2.381 ± 0.051	-3.638 ± 0.167
spSpec-54141-2513-309.fit	8.236 ± 0.049	-1.296 ± 0.065	-0.715 ± 0.095	-1.783 ± 0.102	-2.506 ± 0.114	-3.589 ± 0.353

Continued on next page

Table 2 – continued from previous page

Spectrum name	12 + log O/H	log N/O	log Ne/O	log S/O	log Ar/O	log Cl/O
spSpec-54568-2524-146.fit	8.212 ± 0.040	-1.208 ± 0.055	-0.708 ± 0.073	-1.728 ± 0.088	-2.560 ± 0.104	...
spSpec-54084-2574-323.fit	8.256 ± 0.065	-1.304 ± 0.082	-0.631 ± 0.133	-1.821 ± 0.109	-2.472 ± 0.082	-3.568 ± 0.277
spSpec-54095-2583-062.fit	8.459 ± 0.067	-1.166 ± 0.084	-0.836 ± 0.140	-1.802 ± 0.112	-2.447 ± 0.085	-3.652 ± 0.225
spSpec-54140-2591-226.fit	8.078 ± 0.040	-1.455 ± 0.054	-0.617 ± 0.081	-1.658 ± 0.076	-2.390 ± 0.053	-3.504 ± 0.277
spSpec-54476-2603-512.fit	8.239 ± 0.049	-1.170 ± 0.064	-0.690 ± 0.098	-1.848 ± 0.105	-2.512 ± 0.108	-3.342 ± 0.191
spSpec-54154-2606-474.fit	8.191 ± 0.036	-1.133 ± 0.048	-0.710 ± 0.067	-1.808 ± 0.082	-2.462 ± 0.076	-3.619 ± 0.280
spSpec-54476-2610-421.fit	8.334 ± 0.021	-1.618 ± 0.030	-0.702 ± 0.038	-1.653 ± 0.039	-2.368 ± 0.032	-3.501 ± 0.072
spSpec-54481-2613-507.fit	8.100 ± 0.092	-1.126 ± 0.119	-0.708 ± 0.199	-1.801 ± 0.165	-2.413 ± 0.116	-3.469 ± 0.452
spSpec-54272-2744-090.fit	8.138 ± 0.079	-0.946 ± 0.101	-0.637 ± 0.169	-1.649 ± 0.130	-2.416 ± 0.101	-3.339 ± 0.275
spSpec-54523-2758-062.fit	8.239 ± 0.047	-1.372 ± 0.062	-0.674 ± 0.090	-1.781 ± 0.097	-2.467 ± 0.061	-3.567 ± 0.307

Table 3: He II galaxies coordinates, names.

Spectrum name	Ra	Dec	Other names
spSpec-51602-0266-100.fit	146.0078	-0.64227164	LEDA 27864, SHOC 270
spSpec-51910-0275-445.fit	161.47824	1.06828785	SHOC 308
spSpec-51690-0341-606.fit	200.94775	-1.54776335	LEDA 46812, SHOC 424, UM 570
spSpec-51910-0456-076.fit	42.0664	-8.28791904	SHOC 137
spSpec-51910-0456-306.fit	40.2175	-8.47428513	[BKD2008] WR 70, SHOC 133
spSpec-51959-0550-092.fit	130.12463	47.11952209	[BKD2008] WR 101, HS 0837+4717, SHOC 220, US 1442
spSpec-51999-0553-602.fit	140.23363	52.56786728	Mrk 1416, SHOC 254b, LEDA 26449, SBSG 0917+527
spSpec-52000-0554-190.fit	140.233	52.56870651	Mrk 1416, SHOC 254b, LEDA 26449, SBSG 0917+527
spSpec-51991-0556-011.fit	147.37627	55.57970428	Mrk 22, LEDA 28251, SBSG 0946+558, SHOC 280
spSpec-52238-0566-497.fit	136.37949	3.59177136	...
spSpec-52339-0578-060.fit	161.2408	3.88698697	...
spSpec-52023-0586-433.fit	218.66318	4.26404619	UGC 9380, LEDA 52092, SHOC 471, ZW VIII 436
spSpec-52377-0624-361.fit	244.09808	47.03397751	[BKD2008] WR 122, UGC 10310, LEDA 101538
spSpec-52162-0673-312.fit	336.29221	-0.19801052	...
spSpec-52174-0676-192.fit	342.74701	0.00911507	...
spSpec-52606-0677-533.fit	345.54169	0.82745522	...
spSpec-52346-0876-175.fit	163.29509	50.28144836	Mrk 156, LEDA 200261, SBSG 1050+505, UGC 5998
spSpec-52620-0899-594.fit	138.64565	47.03534317	...
spSpec-52411-0920-575.fit	222.02242	-1.18270004	[BKD2008] WR 182, SHOC 486
spSpec-52409-0955-608.fit	186.27255	61.15313721	[BKD2008] WR 195, LEDA 2816013, SBSG 1222+614
spSpec-52636-0967-540.fit	176.27606	50.30067825	...
spSpec-52668-1158-062.fit	209.96216	57.43971634	Mrk 1486, LEDA 49819, SBSG 1358+576
spSpec-53355-1181-545.fit	52.22226	0.51783353	SHOC 163
spSpec-52703-1194-397.fit	137.61992	7.18832493	LEDA 213577
spSpec-52723-1285-225.fit	208.8569	46.86426163	...
spSpec-52757-1305-269.fit	145.73643	9.47118378	[BKD2008] WR 245
spSpec-52790-1313-423.fit	178.86807	57.66443634	...
spSpec-53088-1324-234.fit	211.11929	54.39799881	NGC 5471, LEDA 165629
spSpec-52762-1325-353.fit	211.12283	54.39646149	NGC 5471A
spSpec-53172-1399-299.fit	227.3924	37.52947617	...
spSpec-53050-1442-599.fit	174.09927	47.15807724	...
spSpec-53091-1464-370.fit	202.86214	41.86341476	...
spSpec-52964-1476-378.fit	333.11224	1.14313805	...
spSpec-53149-1570-021.fit	251.79443	21.0873642	...
spSpec-53166-1615-120.fit	187.70251	12.04522896	LEDA 41360
spSpec-53498-1646-616.fit	222.21675	34.71194077	...
spSpec-53173-1682-003.fit	242.04318	35.46924973	...
spSpec-54266-1725-068.fit	236.43147	8.96704102	...
spSpec-54439-1785-201.fit	132.81522	58.68194962	...
spSpec-53531-1827-503.fit	217.44586	6.72637939	...
spSpec-53734-1975-467.fit	190.95297	32.13715363	...
spSpec-53734-1975-498.fit	190.98624	32.17074203	[BKD2008] WR 462, NGC 4656, UGC 7907
spSpec-53493-2001-146.fit	184.45544	37.86541748	[BKD2008] WR 415
spSpec-53476-2006-404.fit	194.75121	34.84513092	[BKD2008] WR 419, Mrk 59, LEDA 93120, ZW I 49
spSpec-53473-2008-467.fit	175.2812	32.42700577	LEDA 36252, KUG 1138+327
spSpec-53851-2023-263.fit	198.69736	34.88328171	[BKD2008] WR 473, Mrk 450, LEDA 46065, UGC 8323
spSpec-53493-2132-241.fit	215.92865	22.95799637	...
spSpec-53786-2211-486.fit	166.24393	29.13769913	Mrk 36, KUG 1102+294
spSpec-53819-2226-157.fit	180.06873	27.3330574	...
spSpec-53725-2329-536.fit	21.39244	7.99011087	UGC 993, LEDA 5281

Continued on next page

Table 3 – continued from previous page

Spectrum name	Ra	Dec	Other names
spSpec-53741-2366-124.fit	156.01146	21.08056641	[BKD2008] WR 555, LEDA 30483
spSpec-53815-2430-117.fit	133.09048	12.28104401	...
spSpec-54097-2478-370.fit	160.28999	21.36188889	Mrk 724, LEDA 31819
spSpec-53852-2483-254.fit	162.63548	15.63508511	...
spSpec-54174-2494-361.fit	169.44293	17.74019241	...
spSpec-53875-2508-615.fit	177.1703	17.94250488	...
spSpec-53877-2510-560.fit	177.11391	25.76993561	LEDA 36857
spSpec-54174-2588-369.fit	152.74709	15.70653534	...
spSpec-54154-2606-231.fit	202.22066	15.99287796	...
spSpec-54540-2786-084.fit	214.71303	21.04437256	...

Table 4: He II galaxies abundances.

Spectrum name	12 + log O/H	log N/O	log Ne/O	log S/O	log Ar/O	log Cl/O
spSpec-51602-0266-100.fit	7.835 ± 0.021	-1.622 ± 0.033	-0.849 ± 0.038	-1.676 ± 0.044	-2.398 ± 0.042	-3.575 ± 0.169
spSpec-51910-0275-445.fit	8.230 ± 0.025	-1.328 ± 0.034	-0.753 ± 0.047	-1.698 ± 0.045	-2.459 ± 0.048	-3.495 ± 0.121
spSpec-51690-0341-606.fit	7.777 ± 0.030	-1.631 ± 0.106	-0.849 ± 0.047	-1.727 ± 0.110	-2.386 ± 0.116	-3.347 ± 0.204
spSpec-51910-0456-076.fit	7.976 ± 0.021	-1.553 ± 0.030	-0.687 ± 0.036	-1.561 ± 0.038	-2.286 ± 0.034	-3.493 ± 0.110
spSpec-51910-0456-306.fit	7.912 ± 0.028	-1.061 ± 0.044	-0.818 ± 0.047	-1.768 ± 0.093	-2.496 ± 0.096	...
spSpec-51959-0550-092.fit	7.598 ± 0.026	-1.121 ± 0.042	-0.725 ± 0.043	-1.800 ± 0.061	-2.451 ± 0.073	-3.672 ± 0.324
spSpec-51999-0553-602.fit	7.806 ± 0.042	-1.323 ± 0.061	-0.747 ± 0.080	-1.530 ± 0.096	-2.397 ± 0.064	...
spSpec-52000-0554-190.fit	7.913 ± 0.022	-1.552 ± 0.034	-0.781 ± 0.040	-1.640 ± 0.047	-2.430 ± 0.050	-3.472 ± 0.158
spSpec-51991-0556-011.fit	8.044 ± 0.024	-1.437 ± 0.035	-0.828 ± 0.042	-1.463 ± 0.045	-2.274 ± 0.042	-3.552 ± 0.179
spSpec-52238-0566-497.fit	7.855 ± 0.039	-1.396 ± 0.065	-0.787 ± 0.068	-1.615 ± 0.112	-2.330 ± 0.108	...
spSpec-52339-0578-060.fit	7.464 ± 0.027	-1.690 ± 0.079	-0.727 ± 0.043	-1.764 ± 0.082	-2.514 ± 0.100	...
spSpec-52023-0586-433.fit	7.884 ± 0.101	-1.287 ± 0.138	-0.893 ± 0.240	-1.541 ± 0.207	-2.340 ± 0.140	...
spSpec-52377-0624-361.fit	7.981 ± 0.038	-1.560 ± 0.065	-0.689 ± 0.067	-1.521 ± 0.094	-2.332 ± 0.100	...
spSpec-52162-0673-312.fit	7.935 ± 0.034	-1.567 ± 0.057	-0.719 ± 0.060	-1.676 ± 0.098	-2.434 ± 0.095	...
spSpec-52174-0676-192.fit	7.735 ± 0.042	-1.197 ± 0.066	-0.794 ± 0.072	-1.779 ± 0.127	-2.547 ± 0.171	...
spSpec-52606-0677-533.fit	7.651 ± 0.039	-1.680 ± 0.099	-0.733 ± 0.066	-1.789 ± 0.129	-2.477 ± 0.159	...
spSpec-52346-0876-175.fit	8.029 ± 0.027	-1.584 ± 0.042	-0.780 ± 0.051	-1.621 ± 0.069	-2.384 ± 0.064	-3.535 ± 0.296
spSpec-52620-0899-594.fit	8.098 ± 0.027	-1.545 ± 0.038	-0.699 ± 0.052	-1.739 ± 0.065	-2.462 ± 0.064	-3.537 ± 0.232
spSpec-52411-0920-575.fit	8.098 ± 0.025	-1.434 ± 0.037	-0.728 ± 0.043	-1.588 ± 0.055	-2.443 ± 0.055	-3.515 ± 0.185
spSpec-52409-0955-608.fit	8.003 ± 0.023	-1.553 ± 0.038	-0.734 ± 0.040	-1.504 ± 0.052	-2.320 ± 0.048	-3.413 ± 0.177
spSpec-52636-0967-540.fit	7.783 ± 0.058	-1.813 ± 0.134	-0.815 ± 0.113	-1.682 ± 0.191	-2.469 ± 0.258	...
spSpec-52668-1158-062.fit	7.944 ± 0.030	-1.309 ± 0.042	-0.693 ± 0.059	-1.729 ± 0.086	-2.433 ± 0.085	...
spSpec-53355-1181-545.fit	8.191 ± 0.059	-0.844 ± 0.076	-0.830 ± 0.119	-1.655 ± 0.089	-2.376 ± 0.074	...
spSpec-52703-1194-397.fit	7.629 ± 0.033	-1.414 ± 0.051	-0.694 ± 0.065	-1.545 ± 0.070	-2.168 ± 0.068	-3.281 ± 0.266
spSpec-52723-1285-225.fit	7.555 ± 0.044	-1.759 ± 0.240	-0.726 ± 0.067	-1.647 ± 0.137	-2.447 ± 0.205	-3.015 ± 0.202
spSpec-52757-1305-269.fit	8.241 ± 0.023	-1.541 ± 0.032	-0.702 ± 0.045	-1.771 ± 0.045	-2.476 ± 0.045	-3.573 ± 0.125
spSpec-52790-1313-423.fit	7.949 ± 0.024	-1.382 ± 0.036	-0.785 ± 0.041	-1.655 ± 0.055	-2.389 ± 0.053	-3.424 ± 0.152
spSpec-53088-1324-234.fit	7.937 ± 0.022	-1.087 ± 0.030	-0.686 ± 0.044	-1.674 ± 0.045	-2.417 ± 0.045	-3.403 ± 0.123
spSpec-52762-1325-353.fit	7.465 ± 0.019	-1.272 ± 0.028	-0.530 ± 0.037	-1.619 ± 0.031	-2.155 ± 0.029	-3.356 ± 0.080
spSpec-53172-1399-299.fit	7.852 ± 0.028	-1.451 ± 0.052	-0.811 ± 0.045	-1.622 ± 0.070	-2.385 ± 0.077	-3.430 ± 0.197
spSpec-53050-1442-599.fit	7.907 ± 0.030	-1.460 ± 0.052	-0.751 ± 0.050	-1.514 ± 0.069	-2.377 ± 0.080	-3.298 ± 0.186
spSpec-53091-1464-370.fit	7.760 ± 0.029	-1.502 ± 0.057	-0.759 ± 0.049	-1.633 ± 0.077	-2.388 ± 0.088	...
spSpec-52964-1476-378.fit	7.614 ± 0.113	-1.475 ± 0.173	-0.792 ± 0.243	-1.624 ± 0.264	-1.877 ± 0.144	...
spSpec-53149-1570-021.fit	7.749 ± 0.039	-1.489 ± 0.071	-0.757 ± 0.066	-1.620 ± 0.101	-2.494 ± 0.065	...
spSpec-53166-1615-120.fit	7.687 ± 0.032	-1.485 ± 0.061	-0.740 ± 0.055	-1.614 ± 0.082	-2.347 ± 0.101	-3.431 ± 0.381
spSpec-53498-1646-616.fit	7.806 ± 0.074	-1.315 ± 0.116	-0.783 ± 0.133	-1.480 ± 0.185	-2.195 ± 0.105	...
spSpec-53173-1682-003.fit	7.821 ± 0.037	-1.560 ± 0.136	-0.751 ± 0.057	-1.722 ± 0.165	-2.356 ± 0.150	...
spSpec-54266-1725-068.fit	7.748 ± 0.023	-1.512 ± 0.036	-0.764 ± 0.039	-1.777 ± 0.049	-2.477 ± 0.056	-3.612 ± 0.200
spSpec-54439-1785-201.fit	7.843 ± 0.031	-1.309 ± 0.051	-0.765 ± 0.052	-1.686 ± 0.082	-2.452 ± 0.090	...
spSpec-53531-1827-503.fit	8.104 ± 0.036	-1.052 ± 0.050	-0.759 ± 0.065	-1.714 ± 0.095	-2.490 ± 0.092	-3.925 ± 0.762
spSpec-53734-1975-467.fit	7.888 ± 0.025	-1.468 ± 0.040	-0.771 ± 0.046	-1.587 ± 0.057	-2.413 ± 0.061	-3.455 ± 0.205
spSpec-53734-1975-498.fit	8.161 ± 0.029	-1.605 ± 0.045	-0.839 ± 0.051	-1.599 ± 0.066	-2.413 ± 0.068	-3.450 ± 0.215
spSpec-53493-2001-146.fit	8.112 ± 0.029	-1.542 ± 0.041	-0.746 ± 0.052	-1.611 ± 0.055	-2.379 ± 0.055	-3.397 ± 0.138
spSpec-53476-2006-404.fit	8.066 ± 0.019	-1.564 ± 0.028	-0.766 ± 0.034	-1.534 ± 0.033	-2.307 ± 0.030	-3.466 ± 0.075
spSpec-53473-2008-467.fit	7.859 ± 0.028	-1.501 ± 0.044	-0.782 ± 0.050	-1.643 ± 0.070	-2.389 ± 0.073	-3.437 ± 0.273
spSpec-53851-2023-263.fit	8.261 ± 0.019	-1.506 ± 0.026	-0.741 ± 0.037	-1.723 ± 0.034	-2.382 ± 0.031	-3.581 ± 0.081
spSpec-53493-2132-241.fit	7.710 ± 0.034	-1.563 ± 0.065	-0.768 ± 0.058	-1.771 ± 0.106	-2.487 ± 0.130	...
spSpec-53786-2211-486.fit	7.826 ± 0.023	-1.580 ± 0.035	-0.734 ± 0.042	-1.599 ± 0.048	-2.336 ± 0.048	-3.501 ± 0.214
spSpec-53819-2226-157.fit	8.021 ± 0.030	-1.456 ± 0.051	-0.730 ± 0.051	-1.658 ± 0.091	-2.428 ± 0.080	-3.679 ± 0.420
spSpec-53725-2329-536.fit	7.803 ± 0.026	-1.714 ± 0.053	-0.838 ± 0.047	-1.741 ± 0.068	-2.584 ± 0.083	-3.658 ± 0.319

Continued on next page

Table 4 – continued from previous page

Spectrum name	12 + log O/H	log N/O	log Ne/O	log S/O	log Ar/O	log Cl/O
spSpec-53741-2366-124.fit	8.168 ± 0.031	-1.499 ± 0.043	-0.685 ± 0.057	-1.686 ± 0.064	-2.470 ± 0.070	...
spSpec-53815-2430-117.fit	8.120 ± 0.024	-1.428 ± 0.034	-0.675 ± 0.046	-1.750 ± 0.055	-2.498 ± 0.056	-3.716 ± 0.267
spSpec-54097-2478-370.fit	8.157 ± 0.026	-1.601 ± 0.040	-0.773 ± 0.048	-1.576 ± 0.052	-2.341 ± 0.052	-3.482 ± 0.162
spSpec-53852-2483-254.fit	7.938 ± 0.026	-1.435 ± 0.039	-0.743 ± 0.045	-1.671 ± 0.062	-2.478 ± 0.065	-3.574 ± 0.256
spSpec-54174-2494-361.fit	7.991 ± 0.031	-1.556 ± 0.045	-0.691 ± 0.059	-1.570 ± 0.068	-2.388 ± 0.073	-3.541 ± 0.334
spSpec-53875-2508-615.fit	7.967 ± 0.028	-1.552 ± 0.048	-0.730 ± 0.049	-1.662 ± 0.072	-2.468 ± 0.075	-3.578 ± 0.321
spSpec-53877-2510-560.fit	8.102 ± 0.023	-1.544 ± 0.034	-0.790 ± 0.042	-1.771 ± 0.059	-2.609 ± 0.063	-3.441 ± 0.150
spSpec-54174-2588-369.fit	7.931 ± 0.027	-1.427 ± 0.041	-0.731 ± 0.049	-1.678 ± 0.068	-2.468 ± 0.072	-3.497 ± 0.255
spSpec-54154-2606-231.fit	7.761 ± 0.033	-1.431 ± 0.056	-0.761 ± 0.057	-1.539 ± 0.077	-2.314 ± 0.085	...
spSpec-54540-2786-084.fit	7.564 ± 0.028	-1.493 ± 0.052	-0.739 ± 0.045	-1.764 ± 0.071	-2.432 ± 0.087	-3.341 ± 0.197